

Techno-economic evaluation of electricity price-driven heat production of a river water heat pump in a German district heating system

Ulrich Trabert*, Mateo Jesper, Weena Bergstraesser, Isabelle Best, Oleg Kusyy, Janybek Orozaliev, Klaus Vajen.

*Department of Solar- and Systems Engineering, University of Kassel, Kurt-Wolters-Str. 3, 34125 Kassel, Germany

ABSTRACT

Large scale heat pumps (HP) are an important technology that will link district heating (DH) systems to the electricity sector in future smart energy systems. This paper examines the feasibility of the integration of a river water HP at a combined heat and power plant in Germany. It is part of a more extensive study about the transformation of a DH system in an urban district towards a 4th generation DH system. The focus is on operational characteristics and economic efficiency of electricity price-driven heat production. A novel method for estimating the coefficient of performance (COP) of two-stage ammonia HPs based on the difference between sink and source temperature is presented. The HP achieves a seasonal COP in the range of 3.4 to 3.7. The 15-year simulation with the software energyPRO shows that electricity-price driven operation is especially relevant for lower heat loads during the non-heating season. The correlation between volatility of electricity market price change and flexible operation is analysed. Finally, the levelized cost of heat for four designs with heat outputs of the HP from 4.7 MW_{th} to 6.1 MW_{th} and increasing storage sizes are compared. The results indicate that electricity costs are reduced in more flexible systems, but cost parity to the minimum dimensioning is not yet reached with the underlying economic framework conditions. However, the parameters that benefit the economic efficiency of more flexible systems are discussed.

Keywords

Large-scale heat pumps;
Coefficient of performance;
Electricity price-driven operation;
Levelized cost of heat;
Transition to 4GDH;

<http://doi.org/10.5278/ijsepm.6291>

1. Introduction

The German district heating (DH) sector is currently dominated by large heating networks with more than 100 km route lengths, that are primarily supplied by combined heat and power (CHP) plants using fossil fuels like natural gas and coal [1]. The transition of those 2nd or 3rd generation networks towards 4th generation DH systems (4GDH) is inevitable for a sustainable and renewable heating sector.

However, there are still challenges on the way to smart thermal grids [2]. The first is the need for lower network temperatures. Supply temperatures in the range

of 65-70 °C are key to a cost-efficient operation of existing DH systems in the future [3]. Lund et al. [4] even argue that in the medium to long term a supply temperature of 55 °C shows the lowest socioeconomic costs for Denmark, when the replacement and adjustment of building heating systems is considered.

Lower temperatures will lay the ground for large-scale heat pumps (HPs) as an important technology to link the electricity and heating sector in future smart energy systems. In combination with thermal storages, they provide a flexibility option for the electricity sector required for the further integration of variable renewable energies (VRE). [2,5] Taking Norway with its already

*Corresponding author - e-mail: solar@uni-kassel.de

Abbreviations

4GDH	4 th generation district heating
a	fit parameter [-]
AP	assessment period [a]
b	fit parameter [-]
c	fit parameter [-]
C	costs [€]
CC	correlation coefficient [-]
CHP	combined heat and power
COP	coefficient of performance [-]
c_p	isobaric heat capacity [kWh/(kg·K)]
d	fit parameter [-]
DH	district heating
E_t	produced heat in year t [MWh]
EEG levy	renewable energy levy
f_{abs}	fluctuation in electricity market price [€/MWh _{el}]
FLH	full load hours [h/a]
HFC	hydrofluorocarbons
HFO	hydrofluoroolefins
HP	heat pump
k€	thousand €
LCOH	levelized cost of heat [€/MWh]
M€	million €
P_{el}	electric power input [kW]
PV	photovoltaic
\dot{q}	specific heat [kJ/kg]
$Q_{h,use}$	usable thermal energy [kWh]
$Q_{h,out}$	usable heat output [kW]
r	discount rate [-]
R ²	coefficient of determination
R717	ammonia
RV	residual values
SCOP	seasonal coefficient of performance [-]
t	year [a]
T	temperature [K, °C]
\dot{V}_h	volume flow [m ³ /h]
VRE	variable renewable energies
w	work [kJ/kg]
$x_{el,market}$	electricity market price [€/MWh _{el}]

Greek symbols

ΔT	temperature difference [K]
η	efficiency [-]
ρ	density [kg/m ³]
σ	standard deviation

Subscripts

0	evaporation
2 nd	second law of thermodynamics
c	condensation
Carnot	Carnot
el	electric
g	gas cooler
h	heat sink

HP	heat pump
i	time step index
in	inlet
l	heat source
lift	lift
market	market
out	outlet
t	year
th	thermal

highly electrified energy system as an example, Askeland et al. [6] describe the role that the transition towards 4GDH systems can play for increasing efficiency of the electricity system on the one hand and reducing the required electric production capacity on the other.

In an analysis of the role of demand side flexibility for the integration of VRE, Tveten et al. [7] conclude that large commercial consumers like DH plants are more likely to benefit economically from the provision of flexibility for the electricity sector than private households. Moreover, distributed heat storages in DH networks might promote even more flexible operation of DH plants, but Roberto et al. [8] have found that this is merely relevant for systems with non-flexible heat sources like solar heat or waste heat instead of flexible operation units like HP and CHP.

Prina et al. [9] investigate a hybrid electric-thermal solution for an alpine town in Northern Italy by coupling photovoltaic (PV) systems with large HPs and thermal storage in comparison to a renewable system with electric storage. The results indicate that the electric-thermal solution is more cost efficient and should be combined with a grid connection for further improvement.

Knies [10] proposes an integrated heat planning approach for urban environments with high energy demand that includes spatial restrictions, as those are relevant for the interaction of the electricity and heating sector. Local balancing can lead to reduced costs for the electricity grid, especially in cities with a high number of installed PV systems [11].

It has been laid out in previous studies, how the flexible operation of HPs and CHP plants can balance surpluses and deficits in the electricity grid [12–14]. In this context, the software energyPRO [15] is used in multiple studies for energy system analysis as it enables to simulate electricity price driven operation of DH systems in combination with an economic evaluation.

Sneum and Sandberg [16] have analysed the economic framework conditions that would incentivise flexible DH in Finland, Norway, Sweden and Denmark.

They conclude that current taxes and subsidies favour heat production with biomass in CHP or boilers and that a targeted reduction of electricity taxes for large electric boilers is needed for increasing flexibility. Introducing variable taxes for electricity is another approach to promote flexibility, that is pointed out by Østergaard and Andersen [17] in a study about a generic danish DH system supplied by a HP and an electric boiler. Their results indicate that a completely flexible tax of 100 % of the electricity spot market price would indeed incentivise overcapacity in storage volume, but optimal HP capacity only increases slightly.

Nevertheless, the flexible use of HPs in existing DH systems seems to be a viable solution for utilizing renewable heat sources. Rämä and Wahlroos [18] have shown that the integration of HPs is more cost-efficient than solar collectors for the Helsinki DH system at distribution temperatures of 80-110 °C. On the national level, Kontu et al. [19] identify a potential of 10 % to 25 % share of HPs in the DH sales for Finland under the precondition that profitability of the existing DH systems is unchanged or improved.

Bach et al. [20] have studied the role of HPs in the Copenhagen DH system and conclude that the preferred integration is at DH distribution level in order to reach 3,500 to 4,000 full load hours (FLH). Pieper et al. [21] present a methodology to find the optimal amount of HP capacity installed on city level. It was applied to the DH system of Tallinn and included the integration of heat sources like sewage water, river water, ambient air, seawater and groundwater.

Although the literature review demonstrates the benefits that large-scale HPs bring for smart thermal grids on national, regional or city level, practical implementations, particularly in Germany, are rare. According to Popovski et al. [22] the German regulatory and economic framework is currently a barrier for cost parity of HPs in comparison to fossil-fired CHP plants.

The following study deals with a specific opportunity to integrate a river water HP at an existing CHP plant site. The first main aspects to be discussed are seasonal as well as long-term effects of electricity price-driven operation. It is examined how the varying heat demand throughout the year affects the flexible HP operation according to electricity spot market prices at different HP and thermal storage capacities. Moreover, the ongoing integration of VRE into the electricity grid is expected to increase the volatility of electricity market

prices in the long run, which consequently might also influence flexible HP operation.

As the source and supply temperature of the investigated river water HP depend on the season and therefore deviate from nominal operating conditions, a novel approach for HP performance estimation based on the findings of Jesper et al. [23] is introduced. Within the planning process for new HP installations, it is important for the economic evaluation to estimate the performance as accurate as possible, but at the same time with a reasonable effort.

Finally, the impact of flexible HP operation and performance estimation on the cost efficiency of the river water HP of the case study is analysed.

1.1. Feasibility study

The results presented in this paper are embedded in a feasibility study about the transformation of an existing DH network in an urban district in Germany towards 4GDH. Currently, the DH network supplies around 37.8 GWh of heat to the customers per year, which covers 37 % of the total heat demand of the district. The study was conducted in line with the requirements of the German subsidy program “Wärmenetzsysteme 4.0” (heating network systems 4.0), which supports the development of new smart thermal energy networks as well as the transformation of existing DH networks [24].

The central requirement of the program is the integration of at least 50 % of renewable energies into the DH network. Since high temperatures often prevent the integration of renewable heat into existing heating networks, another noteworthy requirement is that the maximum supply temperature must be lower than 95 °C.

In contrast to the main study covering all aspects of the transformation towards a 4GDH system, this paper focuses on the efficient DH integration of a river water HP considering seasonal variations of the temperature of the heat source and sink. Additionally, the software energyPRO [15] is used for the assessment of flexible heat production induced by electricity spot market prices. Finally, the leveled cost of heat (LCOH) for four different system designs are calculated.

1.2. District Heating integration of a river water heat pump at a CHP plant

The district analysed in the feasibility study is a densely populated area in the centre of a large city, thus having limited renewable heat resources. Nevertheless, an adjacent river was identified as the renewable heat source

with the highest potential to cover significant amounts of the heat demand of the district.

The river water is already used for cooling of a CHP plant, which is located in the district and is one major heat source for the DH network of the whole city. This enables to use the existing river water extraction points and permissions at the CHP plant site for the integration of a HP, that feeds the downstream network of the considered district. This part of the network is implemented as a subnetwork separated by a district substation, so that the supply temperature can be lowered compared to the primary DH network.

The electricity for the HP is assumed to be supplied by the CHP plant. The maximum electricity consumption of the HP is below 1 % of the nominal electric load and the maximum heat output of the HP is around 3 % of the nominal thermal load of the CHP plant. Therefore, the CHP operation is seen to be independent of the HP.

A schematic representation of the integration concept is depicted in Figure 1. The river water in the cooling cycle of the CHP plant is partially redirected through a shell-and-tube heat exchanger, where it serves as the heat source of the HP through an intermediate cycle (70 % water, 30 % glycol). As the river water is cooled down by 2 K in the heat exchanger, the minimum river water temperature for HP operation is set to 3 °C to avoid freezing in the subsequent piping leading to the CHP plant.

A tank thermal energy storage connected to the subnetwork serves as the heat sink of the HP. The residual load is covered by the primary DH network through the district substation, which also provides the opportunity of an additional temperature lift.

1.3. Heat pump performance modelling

The economic and environmental feasibility of a HP depends strongly on its performance. The higher the efficiency is, the lower are energy consumption, direct or indirect greenhouse gas emissions and LCOH. The efficiency in turn is strongly influenced by the HP design and the temperatures of the heat source and sink. Therefore, a measured performance map covering all occurring operating conditions is a crucial input for a feasibility study.

Since no performance map is available to this study, an efficiency model that is as accurate as possible is to be used. Therefore, the HP performance model implemented to the employed simulation software energyPRO [15] is evaluated in this chapter. In the next step, a recent study by the authors [23] on market available large-scale HPs is summarized. The results of this study are used to develop a new performance model for the two-stage ammonia HP investigated in this study.

The coefficient of performance (COP) is a commonly used metric for the HP efficiency and compares heat output to electric power input (see Eq. (1)). The HP

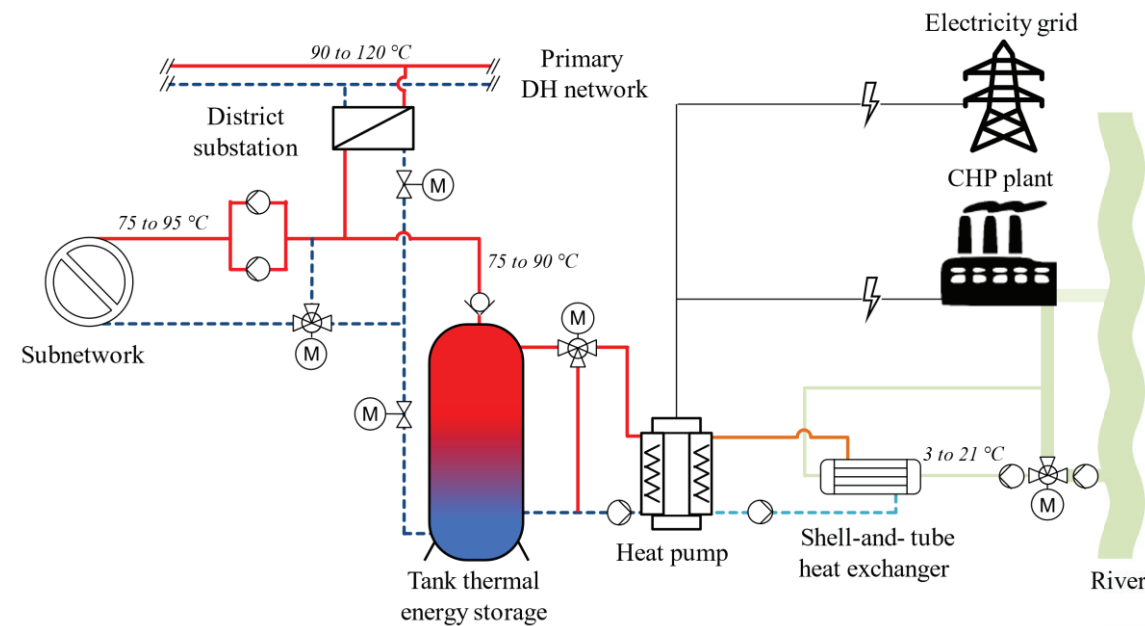


Figure 1: District heating integration of a river water HP (schematic representation)

model implemented to the simulation software energy-PRO [15] is based upon a simple but frequently used method to estimate the COP at a specific operation point. This COP model assumes a constant 2nd law efficiency (η_{2nd}) over the whole operating range.

The 2nd law efficiency is the ratio of the real-world COP and the thermodynamic limit. If evaporation and condensation are isothermal (see Figure 2 left), the anti-clockwise Carnot cycle is the thermodynamic limit and the COP can be estimated using Eq. (2). The latter is the case for most refrigerants used in commercially available mechanical compression HPs.

For HPs with a temperature glide at heat sink or source side, the Lorenz cycle is the thermodynamic limit [25] and the COP can be estimated using Eq. (3). The temperature changes at sink or source side are captured by the logarithmic mean temperature (see Eq. (4) and Eq. (5)) [26]. For instance, HPs using CO₂ are operated transcritical and therefore the transcritical gas is cooled down at heat sink side (see Figure 2 right). This explains

why the logarithmic mean temperature ($T_{h,m}$) should be used for COP calculation. In contrast to that, the evaporation of CO₂ at heat source side is isothermal and therefore no logarithmic mean temperature should be used here ($T_{l,m} = T_{l,in}$) [27]. For both cycles, η_{2nd} includes all efficiency losses resulting, for example, from heat exchanger's temperature driving forces which in turn cause a reduced evaporation temperature (T_0) or an increased condensation temperature (T_c).

$$COP = \dot{Q}_h / P_{el} = [(T_{h,out} - T_{h,in}) \cdot \dot{V}_h \cdot \rho_h \cdot c_{p,h}] / P_{el} \quad (1)$$

$$COP = \eta_{2nd} \cdot COP_{Carnot} = \eta_{2nd} \cdot T_{h,out} / (T_{h,out} - T_{l,in}) \quad (2)$$

$$COP = \eta_{2nd} \cdot COP_{Lorenz} = \eta_{2nd} \cdot T_{h,out} / (T_{h,m} - T_{l,in}) \quad (3)$$

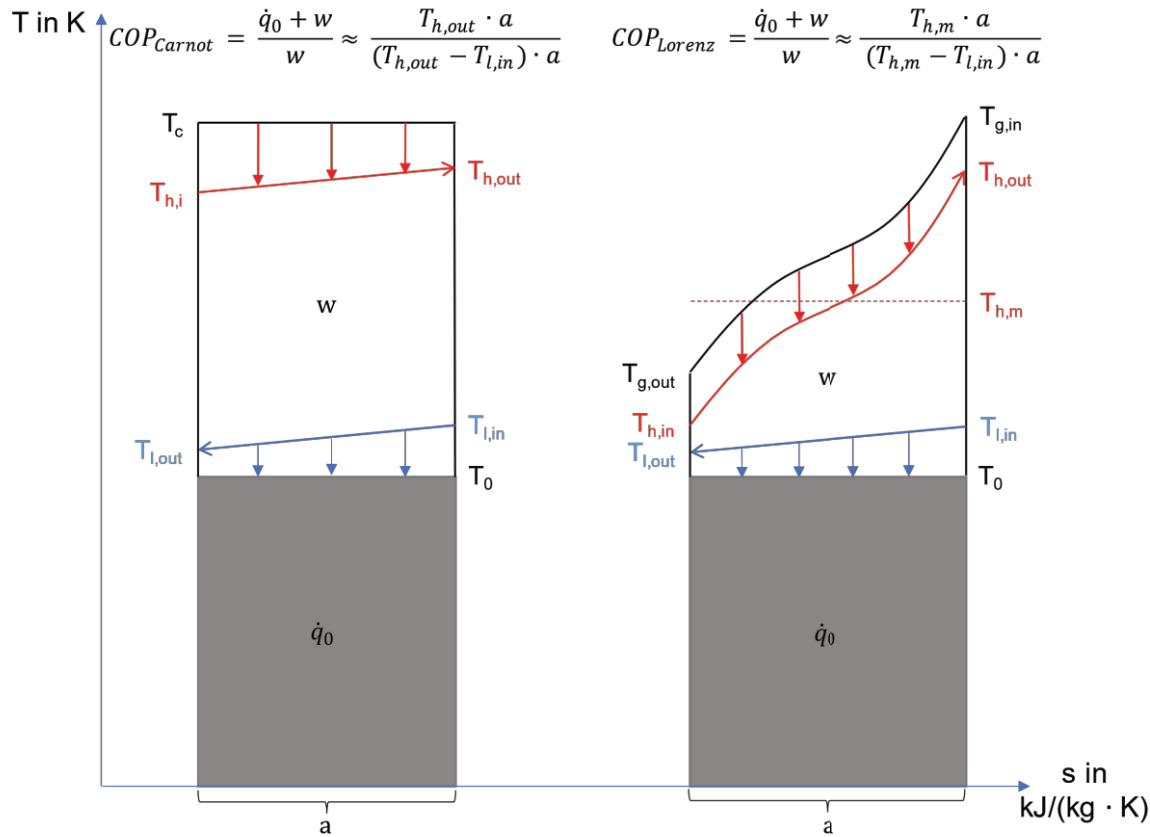


Figure 2: T-s diagram of Carnot cycle HP (left) and Lorenz cycle HP (right) (Lorenz cycle is exemplified by a transcritical operated HP using the refrigerant CO₂; T_c: condensation temperature, T₀: evaporation temperature, T_{g,in}: temperature of refrigerant at gas cooler inlet, T_{g,out}: temperature of refrigerant at gas cooler outlet)

$$T_{h,m} = (T_{h,out} - T_{h,in}) / \ln(T_{h,out} / T_{h,in}) \quad (4)$$

$$T_{l,m} = (T_{l,out} - T_{l,in}) / \ln(T_{l,out} / T_{l,in}) \quad (5)$$

COP	coefficient of performance [-]
\dot{Q}_h	usable heat output [kW]
P_{el}	electric power input [kW]
$T_{h,in}$	heat carrier temperature at condenser inlet [K]
$T_{h,m}$	logarithmic mean temperature at condenser/gas cooler [K]
$T_{h,out}$	heat carrier temperature at condenser outlet [K]
$T_{i,in}$	heat carrier temperature at evaporator inlet [K]
$T_{l,m}$	logarithmic mean temperature at evaporator [K]
$T_{l,out}$	heat carrier temperature at evaporator outlet [K]
\dot{V}_h	volume flow of heat carrier at condenser [m³/h]
η_h	density of heat carrier at condenser [kg/m³]
$c_{p,h}$	isobaric specific heat capacity of heat carrier at condenser [kWh/(kg·K)]

To adapt to a specific HP, energyPRO [15] calculates the 2nd law efficiency at a given operating point and then uses this to estimate the COP for all other operating points. In doing so, energyPRO exclusively uses Lorenz cycle as comparison process (Eq. (3)) [28]. As described above, Eq. (3) is only recommended if there is a temperature glide at heat sink and source side, which is not the case for most mechanical compression HPs available at the market.

Jesper et al. [23] recently found that the 2nd law efficiency depends on the temperature lift between heat source and sink. For market available single-stage compression HPs, the 2nd law efficiency has an optimum for medium temperature lifts around 40 K and is decreasing towards the upper and lower end of the possible operating range. In contrast to the assumption of a constant 2nd law efficiency made in energyPRO, the 2nd law efficiency of these real HPs is varying from around 0.25 to 0.6 [23].

Pieper et al [21] present a modelling framework based on mixed-integer linear programming for planning the integration of large HPs into DH. This study reveals that the 2nd law efficiency of a DH-HP varies significantly over the course of a year depending on the heat source used (air, ground water, sewage water, sea water, lake water, river water). The maximum variation in the range

of 0.50 to 0.61 is observed for air. The minimum variation in the range of 0.55 to 0.58 is obtained for groundwater.

Due to the described inaccuracies of the HP model implemented in energyPRO it is replaced in the simulation results of this study. Therefore, a new performance model for two-stage HPs is developed (section 2.2). This model is based on the results of Jesper et al. [23] and Schlosser et al. [27]. They develop COP regressions for six HP classes based on a comprehensive HP database including operating data of 39 different market available large scale ($> 50 \text{ kW}_{th}$) HP series by 11 manufacturers and propose a function (see Eq. (6)) that leads to a significantly more accurate COP estimation compared to Eq. (2) or Eq. (3).

For single-stage subcritical compression HPs working with hydrofluorocarbons (HFC) or hydrofluoroolefins (HFO), the usage of Eq. (6) instead of Eq. (2) leads to an increase of the coefficient of determination (R^2) from 0.78 to 0.96 and a reduction of standard deviation (σ) from 0.80 to 0.28. For single-stage compression HPs working with ammonia, a R^2 of 0.87 and a σ of 0.42 is achieved [23].

$$COP = a \cdot (T_{h,out} - T_{l,in} + b)^c \cdot (T_{h,out} + 2 \cdot b)^d \quad (6)*$$

COP	coefficient of performance [-]
a, b, c, d	fit parameter [-]
$T_{h,out}$	heat carrier temperature at condenser outlet [K]
$T_{l,in}$	heat carrier temperature at evaporator inlet [K]

*If a temperature glide of the refrigerant at heat sink or source side occurs (e.g. transcritical CO_2 HP), the temperatures in Eq. (6) are replaced by logarithmic mean temperatures.

2. Methodology

The DH integration of large-scale HPs was analysed in terms of operational efficiency and electricity price-driven operation. The methodology to determine key figures including the seasonal coefficient of performance (SCOP) of the HP, indicators for flexible operation and LCOH is laid out in the following subsections.

2.1. Simulation of heat production with energyPRO

A model of the integration concept was developed with the software energyPRO (V4.6.806) [15]. The software enables long-term simulation of DH supply systems on

an hourly basis. Dynamic input variables are integrated as time series and include temperature profiles (ambient temperature, river temperature, supply and return temperature of the DH network), heat demand profiles as well as electricity spot market prices. The simulation period spans over 15 years from the year 2024 until 2038.

The components in the basic version of the model follow a minimum dimensioning approach (see Table 1), meaning that the heat output of the HP is just sufficient to cover 50 % of the annual heat demand of the district, while the capacity of the storage is just large enough to shift peak loads. In the models HP10 to HP30 the heat output of the HP is increased by 10 %, 20 % and 30 %, respectively, while the produced heat and therefore the cover ratios are aimed to stay constant. At the same time the storage volume is increased by 300 m³ in each version. Consequently, the flexibility in the operation of the HP increases from the basic version to HP30.

Table 1: Dimensions of HP and storage in the compared simulation models

Component	Basis	HP10	HP20	HP30
HP	4.70 MW _{th}	5.17 MW _{th}	5.64 MW _{th}	6.11 MW _{th}
Storage	600 m ³	900 m ³	1,200 m ³	1,500 m ³

2.1.1. Temperature profiles

A profile for ambient temperature was generated with the software Meteonorm (Version 7) [29] for the years 2020, 2030 and 2040 within the IPCC scenario A2. Subsequently, a continuous profile for the simulation period was created through linear interpolation between the three support years. The river temperature profile as shown in Figure 3 was built based on the ambient temperature profile. The approximation for river

temperature is a weighted average of the ambient temperatures of the preceding two weeks. The weighting factors were derived from an analysis of historic measured values of ambient and river temperature.

Furthermore, the temperatures of the DH supply and return line were modelled as functions of daily mean ambient temperature as depicted in Figure 4. Those reflect measured supply and return temperatures from the current network adjusted to aspired temperatures in the new subnetwork. The maximum supply temperature was set to 95 °C at an ambient temperature of -10 °C.

2.1.2. Annual heat demand and hourly profile

The annual heat demand of the DH consumers considered in the simulation model relies on a comprehensive study, that builds on consumption and building typology data and was conducted by the utility. The study indicates an annual heat demand of around 37.8 GWh for all DH consumers in the year 2020, but the heat demand is expected to decrease due to renovation measures and increasing ambient temperature in the future. Within the feasibility study it was assumed that the decreasing heat demand is compensated through new consumer acquisition. This is in line with the business strategy of the utility.

Additionally, a new district is expected to be gradually connected to the subnetwork between the year 2025 and 2029, so that the annual heat demand increases to around 50.6 GWh in the year 2030. Standard load profiles from Hellwig et al. [30] and its further development by Hinterstocker et al. [31] were then used to create an hourly load profile in dependence of mean ambient temperature.

The heating network losses were modelled as an hourly load profile using the UA-value and temperature

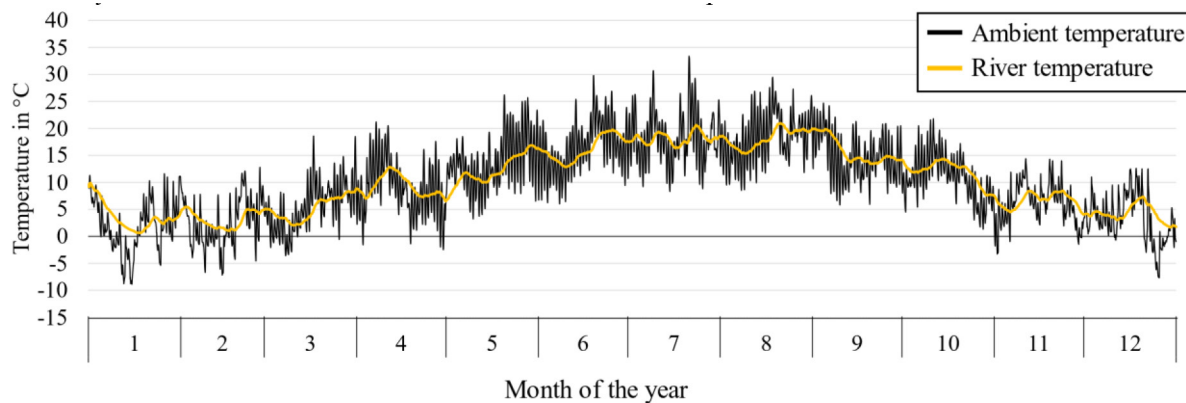


Figure 3: River temperature as a function of ambient temperature for the year 2030

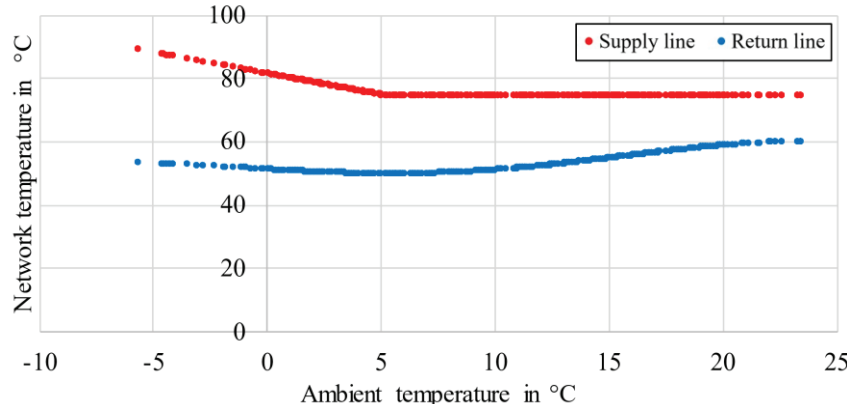


Figure 4: Network temperatures (supply and return line) as a function of ambient temperature

of the network as well as soil temperature as a function of ambient temperature. Those amount to around 5.3 GWh in 2020 and increase to around 7.1 GWh in 2030.

2.1.3. Electricity price-driven heat production

The software energyPRO uses an analytical method to optimize the operation of heat production components and storage according to given technical and economic constraints on an hourly basis [15]. The technical constraints include the performance under nominal operating conditions, partial load restrictions and daily or seasonal limitations on operating hours.

The relevant economic constraints are a long-term prognosis for hourly electricity spot market prices based on energy market models of the company Prognos AG as well as a prognosis for the German renewable energy levy (EEG levy) on electricity according to Oeko-Institut [32]. Considering these restrictions, the operation of the HP will be adapted to electricity market prices, using as many hours at low prices as possible.

The electricity price-driven heat production is described by the following indicators to visualize the effects of short- and long-term development of market prices. The deviation of mean market price during HP operation $d_{el,HP}$ from mean market price $\bar{C}_{el,market}$ is determined on a monthly basis following Eq. (7). The calculation of mean market price excludes hours when the river water temperature drops below 3 °C, because this is the limit for HP operation.

Additionally, the fluctuation of electricity market price is characterised by market price change $f_{abs,i}$ calculated for each time step i as a difference between electricity prices in time steps $i + 1$ and i as in Eq. (8). The corresponding standard deviation $\sigma(f_{abs,i})$ calculated

over a chosen period (e.g. one month) is then used as an indicator for the volatility of the electricity market price change in this period.

Finally, the linear correlation coefficient CC of $d_{el,HP}$ and $\sigma(f_{abs,i})$ is determined to describe how flexible HP operation and price volatility are linked.

$$d_{el,HP} = \frac{C_{el,HP}}{E_{el,HP}} - \bar{x}_{el,market} \quad (7)$$

$$f_{abs,i} = x_{el,market,i+1} - x_{el,market,i} \quad (8)$$

$d_{el,HP}$	deviation of mean market price during HP operation [€/MWh _{el}]
$C_{el,HP}$	cost of electricity for the HP [€]
$E_{el,HP}$	electricity consumption of the HP [MWh _{el}]
$x_{el,market}$	electricity market price [€/MWh _{el}]
$\bar{x}_{el,market}$	mean electricity market price [€/MWh _{el}]
f_{abs}	fluctuation in electricity market price [€/MWh _{el}]
i	time step index [-]
$\sigma(f_{abs,i})$	volatility of electricity market price change over a period [€/MWh _{el}]

2.2. COP estimation for two-stage ammonia heat pumps

The maximum temperature lift that has to be supplied by the HP in the application investigated in this study is 87 K (90 °C – 3 °C). The maximum single-stage temperature lift of market available HPs is 95 K but most HPs are limited to 60 K or less [23]. For these reasons, a two-stage HP with ammonia (R717) as a working fluid is chosen for the application examined in this study.

In addition to the high temperature lift, a two-stage ammonia HP can also handle large differences between supply and return temperature (spread) at heat sink side of more than 20 K. In contrast to that, HPs using organic synthetic refrigerants (e.g. HFO or HFC) are usually operated with heat sink spreads of no more than 10 K and are usually slightly less efficient than ammonia HPs [23]. To be compatible to higher heat sink spreads, HPs using organic synthetic refrigerants must be equipped with additional hydraulic components (e.g. feeding supply stream into return stream).

The COP regressions by Jesper et al. [23] and Schlosser et al. [27] do not cover multi-stage HPs. Therefore, a cascade of two HPs (see Figure 5) is used to approximate a two-stage HP. The COP of each stage is estimated using Eq. (6). The overall COP is then calculated using Eq. (9).

$$\begin{aligned} COP_{cascade} &= \frac{\dot{Q}_h}{P_{el,1} + P_{el,2}} = \frac{\dot{Q}_h}{\frac{\dot{Q}_m}{COP_1} + \frac{\dot{Q}_h}{COP_2}} \\ &= \frac{\dot{Q}_h}{\dot{Q}_h - \frac{\dot{Q}_h}{COP_2} + \frac{\dot{Q}_h}{COP_1}} = \frac{COP_1 \cdot COP_2}{COP_1 + COP_2 - 1} \end{aligned} \quad (9)$$

$COP_{cascade}$ coefficient of performance of HP cascade
[-]

COP_1	coefficient of performance of stage 1
COP_2	coefficient of performance of stage 2
\dot{Q}_h	heat output of stage 2 [kW]
\dot{Q}_m	heat output of stage 1 and heat input to stage 2 [kW]
$P_{el,1}$	electric power input to stage 1 [kW]
$P_{el,2}$	electric power input to stage 2 [kW]

To apply Eq. (9), the total temperature lift supplied by the cascade has to be divided between the two HPs. Figure 6 visualizes the COP of each stage and the total COP of the cascade depending on the division of the temperature lift at the nominal operating point ($T_{h,in} = 50^\circ\text{C}$, $T_{h,out} = 90^\circ\text{C}$; $T_{l,in} = 4^\circ\text{C}$, $T_{l,out} = 2^\circ\text{C}$). Because the COP of each stage mainly depends on the respective temperature lift, the maximum COP of the cascade is reached when the overall temperature lift is almost equally divided. Therefore, it is assumed that each of the stages delivers exactly half of the temperature lift.

One manufacturer's offer for a two-stage ammonia HP was available to the authors of this study. At the nominal operating point (see red cross in Figure 7), the manufacturer reports a COP of 2.8, which is almost 0.4 higher than the COP of the HP cascade. One possible reason to explain this is the single refrigerant circuit of the offered HP. The heat exchanger connecting the two refrigerant circuits of the HP cascade is obsolete which results in a higher efficiency. To adapt the COP estimation to the offered HP, Eq. (9) is extended to allow a horizontal shift with $\Delta T_{lift,shift}$ or vertical shift with COP_{shift} (see Eq. (10)).

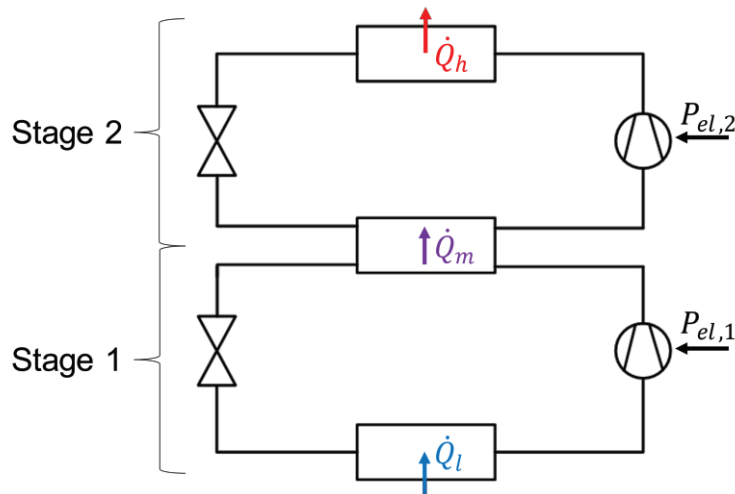


Figure 5: Scheme of a HP cascade.

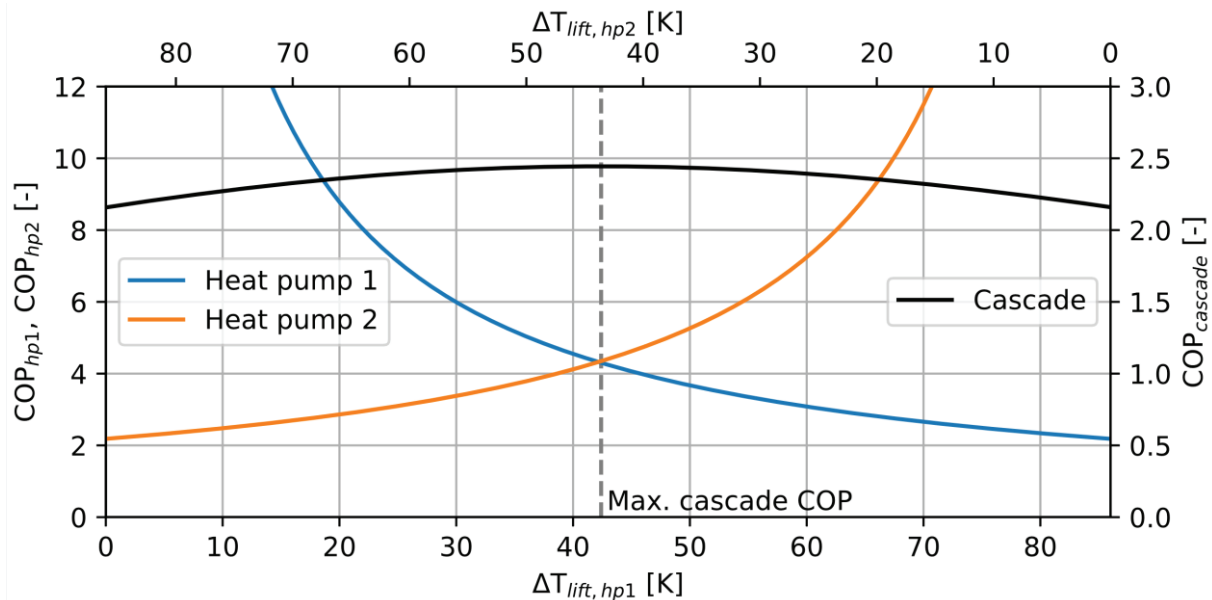


Figure 6: Theoretical COP estimation for a cascade of two ammonia HPs, maximum at $T_{h,out} = 90^\circ\text{C}$ and $T_{l,in} = 4^\circ\text{C}$. COP of cascade reaches maximum at $\Delta T_{lift,hp1} = 42.4$ K and $\Delta T_{lift,hp2} = 43.6$ K ($\Delta T_{lift,cascade} = 90^\circ\text{C} - 4^\circ\text{C} = 86$ K; $\Delta T_{lift,hp1} + \Delta T_{lift,hp2} = \Delta T_{lift,cascade}$).

$$COP_{cascade} = \frac{COP_1 \cdot COP_2}{COP_1 + COP_2 - 1} + COP_{shift} \quad (10)$$

with:

$$COP_1 = a \cdot (\Delta T_{lift,1} - 0.5 \cdot \Delta T_{lift,shift} + 2 \cdot b)^c \cdot (T_{l,in} + \Delta T_{lift,1} - 0.5 \cdot \Delta T_{lift,shift} + b)^d$$

$$COP_2 = a \cdot (\Delta T_{lift,1} - 0.5 \cdot \Delta T_{lift,shift} + 2 \cdot b)^c \cdot (T_{h,out} + b)^d$$

$$\Delta T_{lift,1} = \Delta T_{lift,2} = 0.5 \cdot \Delta T_{lift} - 0.5 \cdot (T_{h,out} - T_{h,in})$$

COP coefficient of performance [-]

COP_{shift} vertical shift of COP function [-]

$$COP_{shift} = 0.37$$

a, b, c, d fit parameter [-]

$$a = 40.789, n = 1.0305, c = -1.0489,$$

$$d = 0.29998 \text{ [23]}$$

$T_{h,out}$ heat carrier temperature at condenser outlet [K]

$T_{l,in}$ heat carrier temperature at evaporator inlet [K]

$\Delta T_{lift,shift}$ horizontal shift of COP function [K]

$$\Delta T_{lift,shift} = 12.8$$

A horizontal shift ($\Delta T_{lift,shift}$), which is equal to a constant reduction of temperature lift, leads to higher COP at low temperature lifts (see Figure 7) and can be physically explained by the missing intermediate heat exchanger. The offered HP is equipped with an internal

heat exchanger, flash tank, desuperheater, subcooler and oil coolers for each compressor. These features are not a standard to all ammonia HPs and are assumed to result in a vertical shift COP_{shift} . Therefore, it is reasonable to assume that the real COP will be located between the horizontally and vertically shifted COP curve. The shifted COP curves are used in the following to mark the estimated COP range resulting from adapting the COP estimation of the HP cascade to a two-stage HP with a single refrigerant circuit.

As the HP performance varies with changing operating conditions, both electrical power consumption and heat output are affected. The behaviour of a specific HP depends on a wide range of parameters such as the properties of the refrigerant. The simple HP performance model implemented in energyPRO and described above is not able to represent this behaviour correctly. To avoid resulting errors and to reduce the complexity of the system control, a constant heat output of the HP is assumed in this study. Since the offered HP is equipped with a built-in frequency converter, a constant heat output can also be achieved in practice.

2.3. Boundary conditions for the economic evaluation

The key indicator used for economic evaluation in this study is the LCOH, which is defined in Eq. (11) by fol-

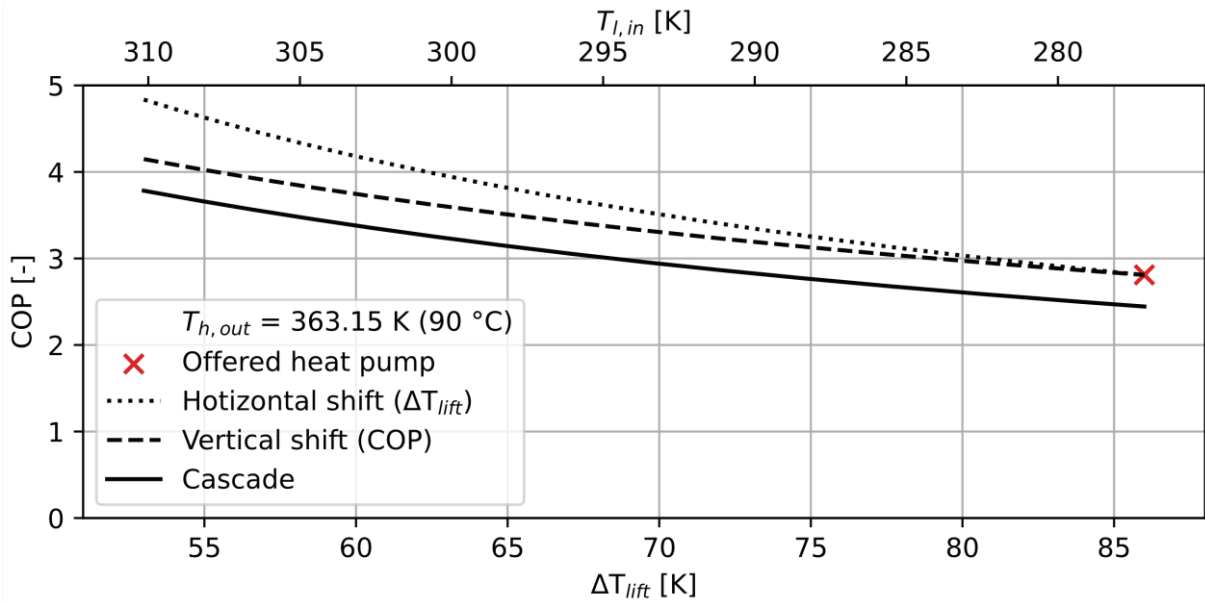


Figure 7: Adaption of the COP curve of a HP cascade to the offered two-stage HP. (Maximum heat source (river) temperature is 21 °C. Because heat source temperature increases and sink temperature decreases in summer, the minimum temperature lift is 54 °C. Vertical shift is 12.8 K. Horizontal shift is 0.37)

lowing Baez et al. [33]. It contains investment costs (I), operating costs for electricity, maintenance and service (C_t) as well as residual values (RV) of the components. The residual values are relevant because the assumed technical lifetime is 20 years for the HP and 25 years for the storage in line with Große et al. [34], while the assessment period (AP) is only 15 years. The transactions for C_t and RV , that occur later than the investment, are discounted to the time of investment with the discount rate (r). Finally, all costs are referred to the produced heat (E_t) to calculate LCOH.

$$LCOH = \frac{I + \sum_{t=1}^{AP} \frac{C_t - RV}{(1+r)^t}}{\sum_{t=1}^{AP} \frac{E_t}{(1+r)^t}} \quad (11)$$

$LCOH$	levelized cost of heat [€/MWh]
I	investment costs [€]
t	year [-]
AP	assessment period, 15 a [-]
C_t	operating costs in year t [€]
RV	residual values [€]
r	discount rate [-]
E_t	produced heat in year t [MWh]

The key assumptions for calculating the LCOH are listed in Table 2. Große et al. [34] list references for investment, maintenance and service costs of the HP and storage. Additionally, the references for investment costs were enhanced by quotes of manufacturers for a two-stage ammonia HP and a river water shell-and-tube heat exchanger to increase the accuracy of the cost estimation. This leads to specific turn-key investment costs for the HP that are within the range of costs for HPs listed by the Danish Energy Agency and Energinet [35] (sea-water HPs) and Große et al. [34]. All assumptions are without value added tax (VAT). A 30 % subsidy is applied to the investment costs according to the German program “Wärmenetzsysteme 4.0” (heating network systems 4.0) [24].

It is assumed that the electricity for the HP is self-generated at the CHP plant. Therefore, the electricity costs only reflect the lost revenue from a potential sale of CHP electricity at a spot market. In this setup, according to German legislation, the only additional fee that needs to be considered is 40 % of the EEG levy (renewable energy levy).

Since the economic assumptions reflect the individual conditions of the conducted case study, the influence of the discount rate and the investment costs on LCOH is tested in a sensitivity analysis. The discount rate is

Table 2: Key economic assumptions

Component	Basis	HP10	HP20	HP30
HP				
<i>Turn-key investment costs</i>	2.74 M€	2.97 M€	3.20 M€	3.44 M€
<i>Maintenance and service</i>	Fix: 2,700 €/(a • MW _{th}); Variable: 1,80 €/(a • MWh _{th})			
Storage				
<i>Turn-key investment costs</i>	0.49 M€	0.75 M€	0.99 M€	1.24 M€
<i>Maintenance and service</i>	12.0 k€/a	13.0 k€/a	14.0 k€/a	15.0 k€/a
Mean electricity market price		58.3 €/MWh _{el} (2024) to 72.8 €/MWh _{el} (2038)		
EEG levy		58.9 €/MWh _{el} (2024) to 13.6 €/MWh _{el} (2038)		
Discount rate r			8 %	
Subsidy			30 % of investment costs	

varied in the range of 0 % to 12 %, while the investment costs are altered by ±30 %.

3. Results of the Techno-Economic Analysis

In the following the simulation results of the integration of a river water HP are presented. The effects of increasing HP output and storage capacity in the four simulation models are examined regarding the overall performance with a focus on HP efficiency and electricity price-driven operation. The analysis concludes with an economic comparison.

3.1. Simulation results

The 15-year simulations of heat production with the energyPRO software provide the basis for the techno-economic analysis. A selection of resulting key figures is listed in Table 3. The cover ratio of the HP is maintained at approximately 52 % of the district heat demand in all models as intended. This is achieved by setting individual maximum electricity market prices for HP operation in each year and each model.

The increasingly flexible operating strategy from the Basis model to HP30 is reflected in a decreasing number of FLH and storage cycles. Nevertheless, the number of FLH is higher than in comparable studies, where it

ranges from 2,000 to 4,000 [20,21]. The deviation may be explained by the HP operation as baseload units in this study in comparison to investigations on city level in the mentioned references, where CHP plants serve as baseload units. It is also notable that larger storage volumes in HP10 to HP30 lead to less hours of the HP below nominal load.

To visualize seasonal operation characteristics, Figure 8 shows the hourly heat load, HP operation and storage utilisation for the models Basis and HP30 in the year 2030. For the reasons described in section 1.3, the heat output of the HP is set to fixed values for the respective scenarios ranging from 4.70 MW to 6.11 MW.

The lowest possible river temperature for HP operation is 3 °C. The periods below this threshold can be seen in the Basis model in January, February, and December, when the HP is not running. Beyond that, operation is restricted in periods with high electricity prices, especially in the model HP30 with a higher heat output. From May until October, when the heat load is lower than the heat output of the HP, this characteristic intensifies through storage utilisation. The comparison of the two models clearly shows that larger capacities in HP30 increase the flexibility in the summer and extend the periods with flexible operation.

Table 3: Key figures of the simulation: Cover ratio, FLH and storage cycles

Key figure	Basis	HP10	HP20	HP30
Mean cover ratio HP	51.6 %	52.0 %	52.5 %	52.6 %
Mean operating hours HP	6,354 h/a	5,668 h/a	5,199 h/a	4,794 h/a
Mean hours below nominal load HP	972 h/a	580 h/a	433 h/a	356 h/a
Mean FLH HP	5,904 h/a	5,418 h/a	5,011 h/a	4,636 h/a
Mean storage cycles	224 a ⁻¹	196 a ⁻¹	175 a ⁻¹	160 a ⁻¹

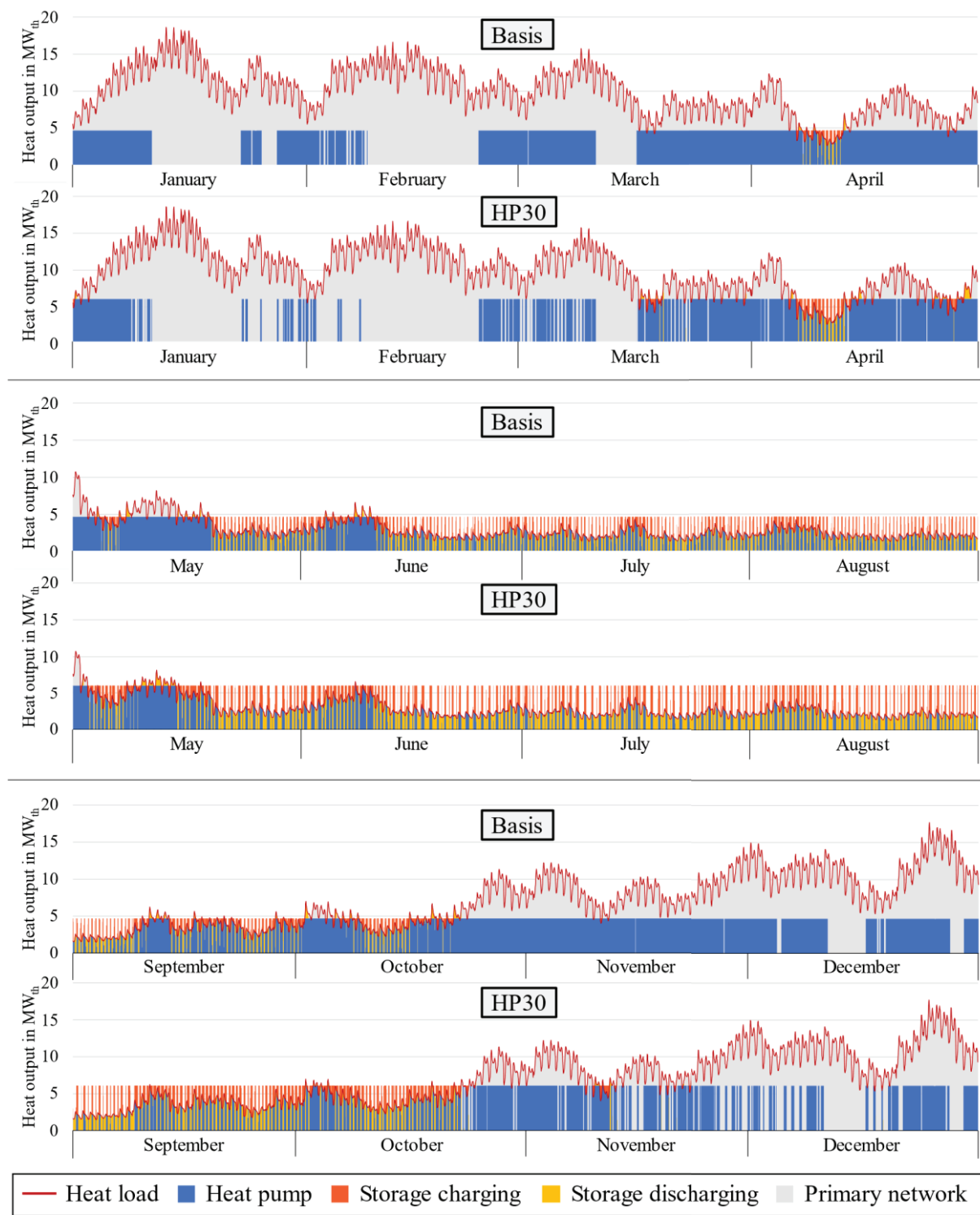


Figure 8: Comparison of hourly simulation results for the year 2030 as course of the year for the models Basis and HP30

3.2. Analysis of electricity price-driven operation

The following section disregards the simulation results for years 2024 to 2029, as the increasing heat load due to a network expansion (see section 2.1.2) may affect conclusions regarding electricity price-driven operation.

In general, the observations made in section 3.1 are confirmed when looking at the monthly development of the deviation of mean market price during HP operation $d_{el,HP}$ depicted in Figure 9 for all four models. From April until the summer, when the heat load is low, the deviation decreases while at the same time the volatility of electricity market price change $\sigma(f_{abs})$ slightly

increases. Depending on the model, the HP is operated when the electricity price is 3 to 23 €/MWh_{el} below mean market price during the summer.

Furthermore, large deviations are observed in December and February especially in models HP10 to HP30. This is explained by a lower number of operating hours compared to the Basis model and by very high peaks in electricity market price during these months.

The progressing decarbonisation of the German electricity system with a growing share of VRE is expected to further increase the volatility of electricity market price change $\sigma(f_{abs})$ in the long-term. Figure 10 shows

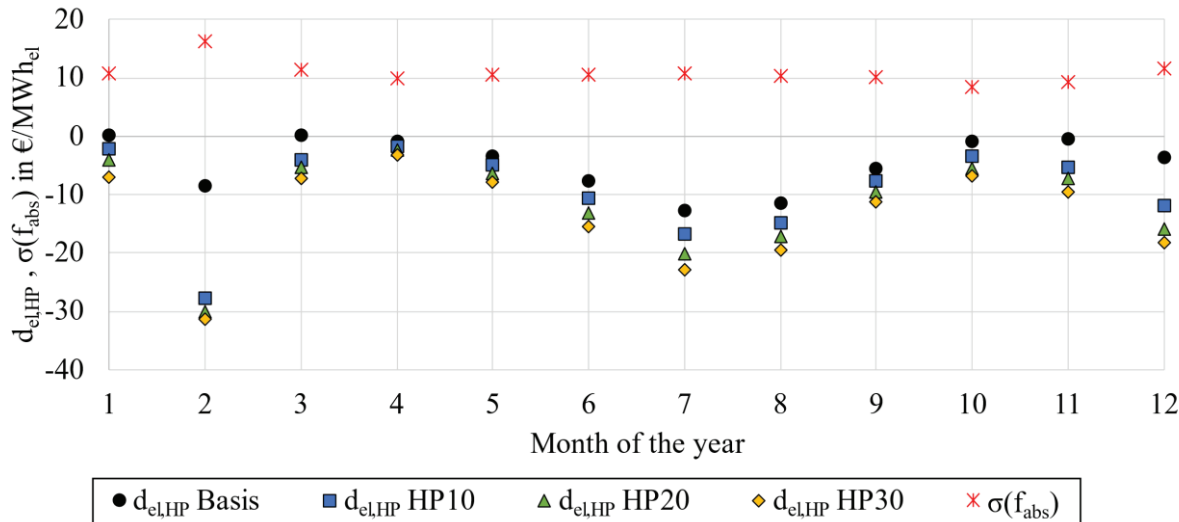


Figure 9: Deviation of mean market price during HP operation $d_{el,HP}$ and volatility of electricity market price $\sigma(f_{abs})$ as course of the year (mean values for the years 2030 to 2038)

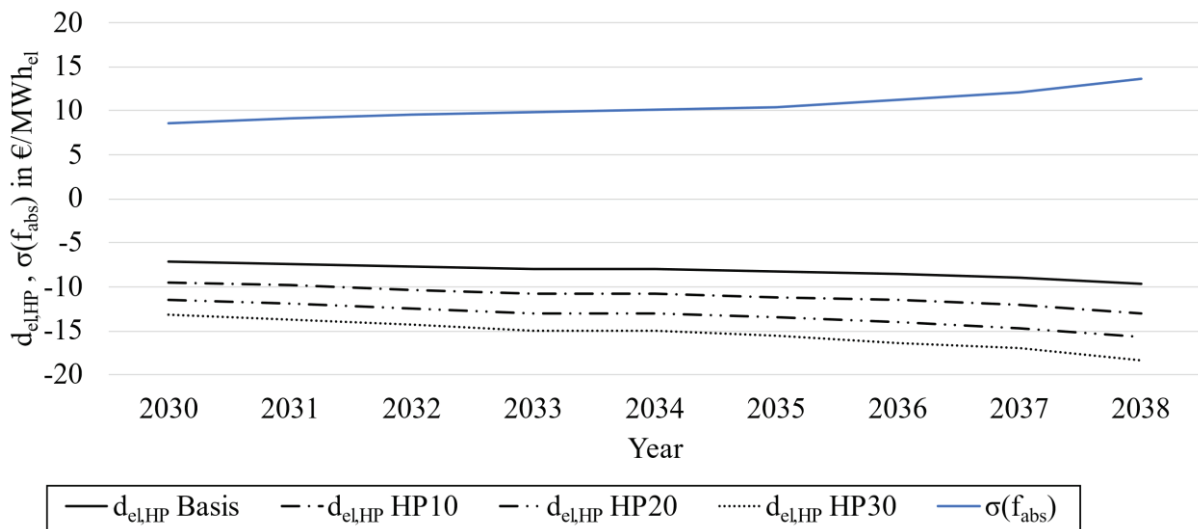


Figure 10: Mean values of the deviation of mean market price during HP operation $d_{el,HP}$ and the volatility of electricity market price $\sigma(f_{abs})$ in the non-heating season (May to September)

that this is specifically the case for the non-heating season (May to September) in the underlying spot market prognosis, which indicates a strong growth of solar PV systems feeding into the electricity grid. The simulation results show that volatility impacts the mean deviation $d_{el,HP}$ with an increasing effect from the Basis model to HP30.

The trend of an increasing volatility $\sigma(f_{abs})$ until 2038 cannot be recognized during the heating season (see Figure 11). Nevertheless, the impact of volatility on the mean deviation $d_{el,HP}$ is also confirmed here, especially in HP10 to HP30.

To further differentiate the impact of volatility $\sigma(f_{abs})$ on mean deviation $d_{el,HP}$, the linear correlation coefficient

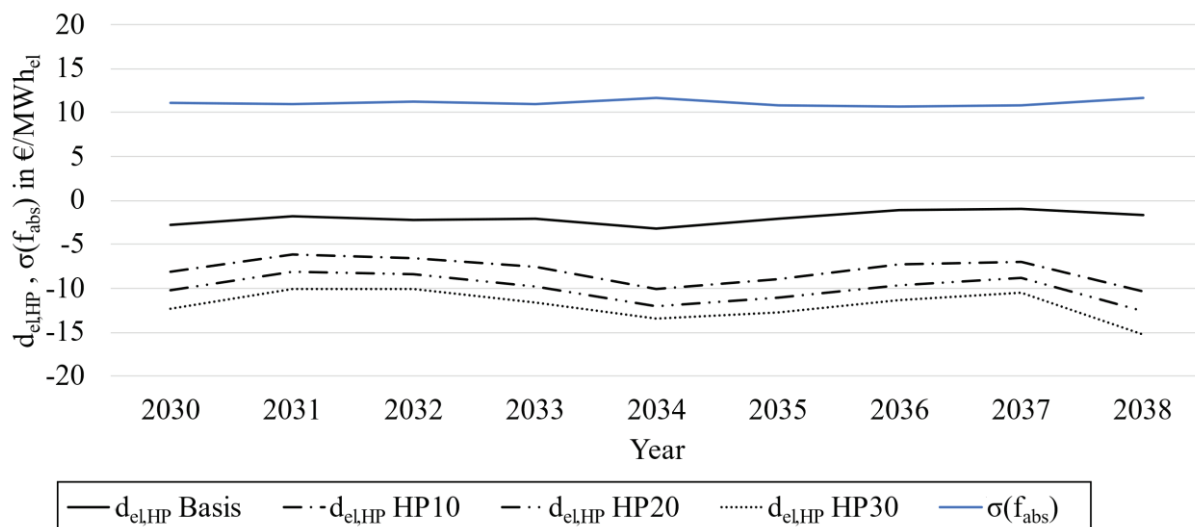


Figure 11: Mean values of the deviation of mean market price during HP operation $d_{el,HP}$ and the volatility of electricity market price $\sigma(f_{abs})$ in the heating season (October to April)

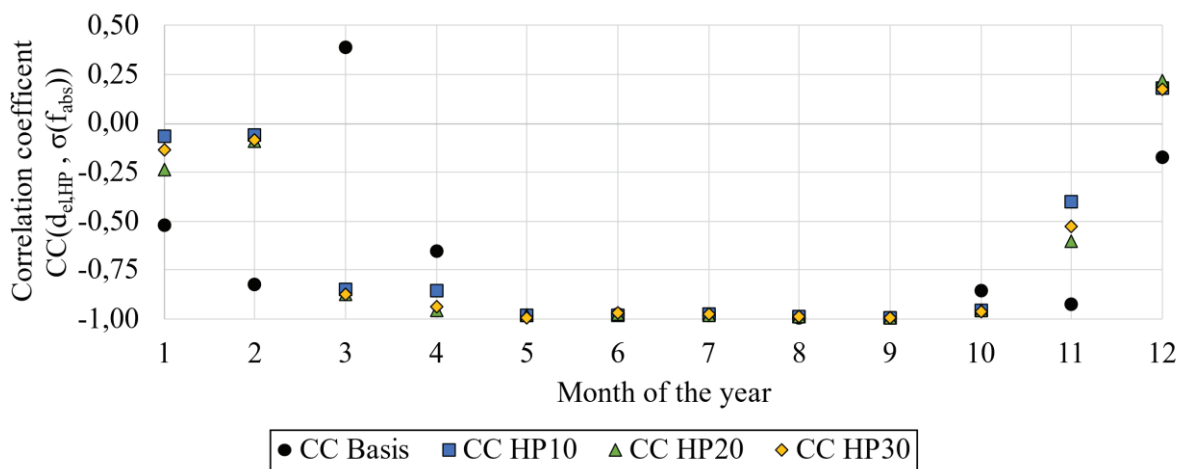


Figure 12: Correlation coefficient of the development of the deviation of mean market price during HP operation $d_{el,HP}$ and the volatility of electricity market price $\sigma(f_{abs})$ for the years 2030 to 2038 as course of the year

CC between their respective long-term developments (for years 2030 to 2038) was determined for each month (see Figure 12). CC is close to -1 from May to September in all models, which demonstrates that an electricity price-driven operation of the HP is particularly possible during the non-heating season. With higher heat output of the HP and additional storage capacity in HP10 to HP30, this period can be extended from March to October. In winter high electricity price peaks, the minimum river water temperature for HP operation and a higher heat load affect heat production more significantly. Consequently CC is less informative for this period.

3.3. Evaluation of heat pump performance model

In section 2.2, two approaches ($\Delta T_{lift,shift}$ and COP_{shift}) are proposed to adapt the method of COP estimation to a two-stage HP with a single refrigerant circuit by representing it with a HP cascade. Figure 13 visualizes the COP of both approaches as well as the Lorenz COP calculated according to Eq. (3) with a constant η_{2nd} of 0.515 for one year. Interruptions in the COP profile indicate times where the HP is out of operation due to river temperatures below 3 °C. This is the case for 11 % of the whole year.

In comparison to the Lorenz COP, the profiles of the proposed estimation methods are independent of the return temperature of the DH network. This is especially relevant during the summer when the DH supply temperature is constant and the COP for both approaches only depends on the river temperature. Nevertheless, $\Delta T_{lift,shift}$ leads to a significantly higher COP in summer when the temperature lift decreases and the operating conditions deviate most from the conditions at the nominal operating point. The maximum deviation of the proposed estimation methods from Lorenz COP is 0.9 (+24 %) for $\Delta T_{lift,shift}$ and 0.35 (+11 %) for COP_{shift} .

The seasonal coefficient of performance (SCOP), which is determined through dividing the annual heat production by the electricity consumption, is 3.3 when using the Lorenz COP. On the other hand, a SCOP of 3.4 is obtained with COP_{shift} and 3.7 with $\Delta T_{lift,shift}$. This corresponds to a range of 9 % deviation between the proposed approaches. In all cases, the dimensioning

(Basis, HP10, HP20, HP30) has no significant influence on the SCOP.

The possible SCOP range of 9 % could be reduced and the accuracy could be increased if more operating points for the offered HP would be available making a simultaneous horizontal ($\Delta T_{lift,shift}$) and vertical (COP_{shift}) adaption possible. In this case, the resulting COP curve (see Figure 7) or annual COP profile (see Figure 13) is assumed to be between the horizontal and vertical shift. In any case, the error resulting from the inaccuracy of the single-stage ammonia HP COP regression ($\sigma = 0.42$; $R^2 = 0.87$), which is taken from Jesper et al. [23] and is a crucial part of the COP estimation of the HP cascade, cannot be eliminated.

3.4. Economic evaluation of heat supply concepts

The LCOH of the four models are compared in Figure 14 including both approaches to adapt the COP estimation method to the offered two-stage ammonia HP ($\Delta T_{lift,shift}$ and COP_{shift}). The use of COP_{shift} leads to about 4 to 5 % higher LCOH compared to $\Delta T_{lift,shift}$. Consequently, the overall economic efficiency of the concept is only slightly affected by the estimation method. In the following only the results with $\Delta T_{lift,shift}$ are discussed.

In general, the electricity-price driven operation of the HP reduces the cost of electricity at a spot market compared to a continuous HP operation. The range of this cost reduction is from 8 % in the Basis model up to 19 % in HP30. Although the LCOH in the Basis model are lowest,

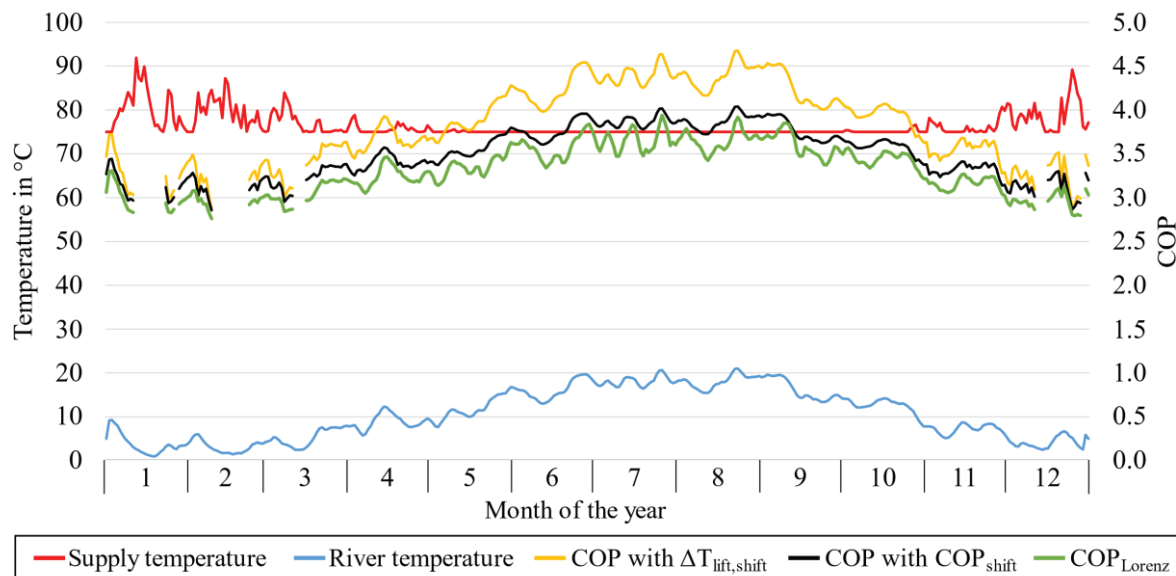


Figure 13: Seasonal profile in the year 2030 of supply temperature, river temperature, COP with $\Delta T_{lift,shift}$, COP with COP_{shift} and COP_{Lorenz}

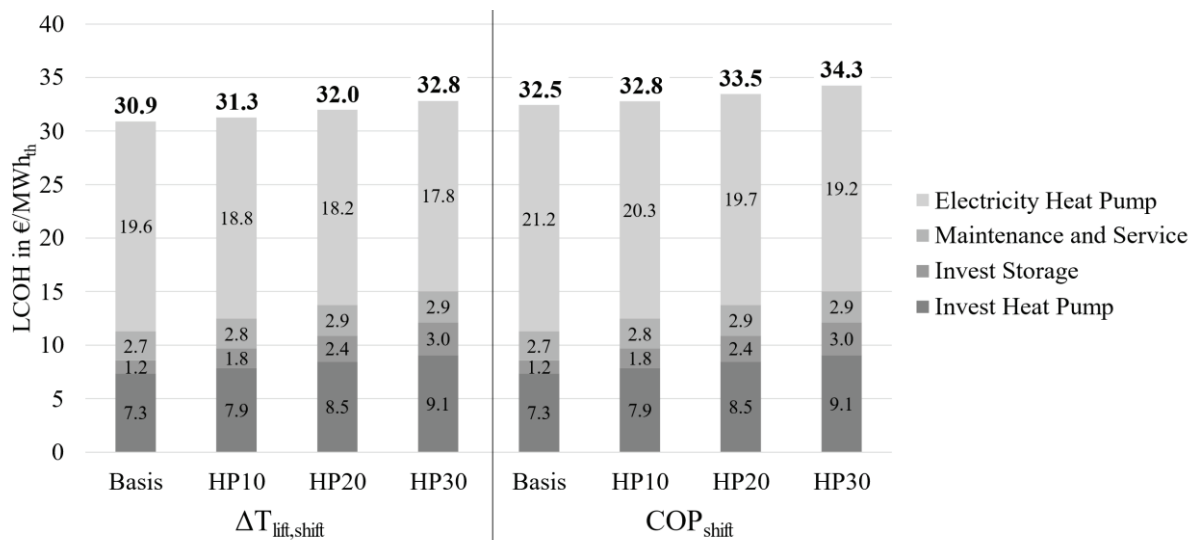


Figure 14: Comparison of LCOH of the Basis, HP10, HP20 and HP30 models for COP estimation with $\Delta T_{\text{lift,shift}}$ and $\text{COP}_{\text{shift}}$

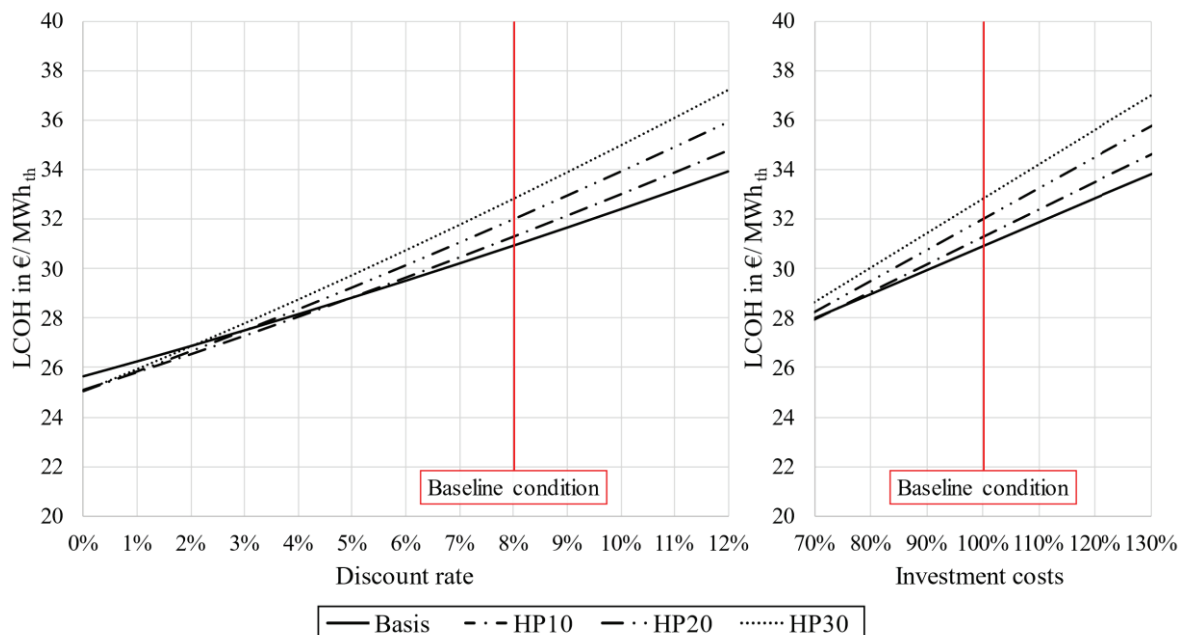


Figure 15: Sensitivity analysis of LCOH for different discount rates (left) and investment costs (right)

a more flexible heat production in HP10 to HP30 increases the LCOH only up to 6 %. With the underlying economic framework conditions, 9 % lower electricity costs in HP30 compared to the Basis model cannot compensate additional investment costs for larger components.

It is important to note here that a precondition of the LCOH calculation is the use of self-generated electricity from the CHP plant. Considering additional fees for grid electricity almost doubles LCOH to 59.2 €/MWh_{th} in the Basis model and 61.0 €/MWh_{th} in HP30.

In order to test the impact of the economic framework parameters on LCOH calculation, a sensitivity analysis for the discount rate and investment costs was conducted. Figure 15 (left) shows that the chosen discount rate is a decisive parameter when comparing the four models. Lower discount rates favour concepts with high investment costs, so that HP10 model has lower LCOH than the Basis for discount rates below 5 % already. Within the range of deviations in investment costs of ±30 % the LCOH of the Basis model stay lowest

(see Figure 15 right), although the differences between the four models are marginalized for decreasing investment costs.

4. Discussion

The integration of a river water HP at a CHP plant bears the opportunity to use existing infrastructure for the transformation of heating networks towards 4th generation DH systems. The reduction of supply and return temperatures of the network is a major precondition that has not been covered in this study but is essential for a successful and efficient implementation. Ommen et al. [3] have shown the positive impact of reduced network temperatures on costs, fuel consumption and carbon emissions and recommend supply temperatures of 65–70 °C, which is slightly lower than the 75–95 °C temperature curve assumed in this study.

As the focus of this investigation is on long-term development, some simplifications within the simulation model were accepted. The proposed integration of the HP with the subnetwork and the primary network requires a well-designed control strategy. In this context the frequent on-and-off operation of the HP as a consequence of electricity price-driven operation may be challenging. Meesenburg et al. [36,37] suggest that two-stage ammonia HPs are able to operate very flexibly and propose several measures to optimize regulation time. In addition, the impact on the upstream network can be reduced by flattening the feed-in profile of the HP through further usage of the storage in winter.

Jesper et al [23] show that the COP of single-stage ammonia HPs can be estimated just using heat sink and source temperatures resulting in a standard deviation σ of 0.42 and a coefficient of determination R^2 of 0.87. In the present study this method is transferred to two-stage ammonia HPs which results in an additional inaccuracy of 0.3 SCOP-points. This inaccuracy could be reduced if more real operating points would be available. In contrast to many methods found in literature (e.g. Ommen et al. [38]) one major advantage of the developed method for COP estimation of two-stage HPs is that it needs no inputs other than heat sink and source temperatures. Every additional input, for example assuming the compressor efficiency, can be a source of error. As the developed method considers a 2nd law efficiency depending on operating temperatures, it is at the same time assumed to be more accurate than comparable methods based on Carnot or Lorenz COP and a constant 2nd law efficiency,

which, for example, is used by the simulation software energyPRO [15]. But since no performance map of a two-stage ammonia HP is available to this study, the latter cannot be validated.

Previous studies have shown that the flexible use of electricity for heat production in DH systems facilitates the progressing integration of VRE into the electricity grid [39–41]. This is confirmed in this study by strong correlation between volatility of electricity market price change and flexible HP operation, but the results also demonstrate how the seasonality of heat load affects the flexibility. However, it should be noted that both the volatility and the level of electricity spot market prices strongly depend on the future development of power plant capacities and the growth of VRE. Since this is subject to many uncertainties such as political decisions on subsidies, carbon taxes, and the regulatory framework, further work should consider different scenarios for the future of the electricity market and show their implications on the present study.

The LCOH of the proposed HP integration models indicate that the initial economic framework parameters favour the minimum dimensioning approach to reach the goal of a 50 % HP cover ratio. However, increased flexibility of the system reduces electricity costs, which present the largest share of the LCOH. Their share is even larger when using grid electricity instead of self-generated electricity. Currently, electricity grid charges are a fixed price component in Germany, but Kirkerud et al. [40] have stressed the importance of time-varying grid charges for flexible use of electricity in the heating sector. Finally, the share of investment costs in the LCOH increases for very flexible systems, so that they are more sensitive to the choice of case-specific discount rates, optimized component dimensions and accuracy of investment cost estimations. The above aspects could make more flexible systems also more economically efficient.

5. Conclusion

A concept for the integration of a river water HP at a CHP plant site was presented designed to cover 50 % of the heat demand of a heating network in an urban district in Germany. The simulation software energyPRO was used to model four different dimensioning approaches aimed at increasing the flexibility of heat production. The models considered decisive constraints for the HP including seasonal and long-term trends for river water

and DH supply temperature, a novel methodology for COP estimation as well as a prognosis for electricity market prices. The results of the 15-year simulation period were then used for evaluating the economic efficiency of the flexible HP operation.

The developed two-stage HP performance model substitutes a performance model implemented to energyPRO that is inappropriate for most market available HPs. Available highly accurate physical HP models from literature need to specify various parameters. In contrast, the developed model is based on empirical correlations and can be applied without the need of additional information. At the same time, the achieved accuracy of the employed empirical correlations is a significant improvement on previous performance models such as the one implemented to energyPRO.

Depending on the model the HP reaches 4,600 to 5,900 FLH. The operation at low electricity market prices is particularly achieved when the heat load is low during the non-heating season and increases with the rising volatility of electricity market price. At a mean supply temperature of 76 °C and a mean river temperature of 10 °C, the SCOP is estimated to be in the range of 3.4 to 3.7, whereas about 11 % of the year the HP is out of operation due to low river water temperature.

The model comparison indicates that lower electricity costs due to more flexibility do not lead to lower LCOH under the assumed economic framework conditions. Nevertheless, there is only a slight gap towards cost parity of the more flexible systems in comparison to the minimum dimensioning approach in the Basis model. For this model, the LCOH is 30.9 €/MWh_{th}, while it is only 6 % higher in the most flexible HP30 model. The discount rate has proven to be a decisive parameter in the context of this evaluation. This gap becomes even smaller, when the HP is operated with grid electricity instead of self-generated electricity from the CHP plant. That is why time varying electricity grid charges are seen as an important regulatory instrument to incentivise more flexible HP operation, that will support the integration of large amounts of VRE into the electricity grid in the future.

6. Acknowledgements

The authors would like to acknowledge the special issue of the International Journal of Sustainable Energy Planning and Management and thank the organisers of

the 6th International Conference on Smart Energy Systems from 6-7 October 2020 originally planned in Aalborg, Denmark, especially for switching to an online conference on short notice. [42]

References

- [1] Schweikardt S, Didycz M, Engelsing F, Wacker K. Sector Study District Heating. Bonn: Bundeskartellamt; 2012 (in German); Available from: http://www.bundeskartellamt.de/SharedDocs/Publikation/DE/Sektoruntersuchungen/Sektoruntersuchung%20Fernwaerme%20-%20Abschlussbericht.pdf?__blob=publicationFile&v=3.
- [2] Lund H, Werner S, Wiltshire R, Svendsen S, Thorsen JE, Hvelplund F et al. 4th Generation District Heating (4GDH). Energy 2014(68):1–11. <https://doi.org/10.1016/j.energy.2014.02.089>.
- [3] Ommen T, Markussen WB, Elmgaard B. Lowering district heating temperatures – Impact to system performance in current and future Danish energy scenarios. Energy 2016(94):273–91. <https://doi.org/10.1016/j.energy.2015.10.063>.
- [4] Lund R, Østergaard DS, Yang X, Mathiesen BV. Comparison of Low-temperature District Heating Concepts in a Long-Term Energy System Perspective. International Journal of Sustainable Energy Planning and Management 2017(12):5–18. <https://doi.org/10.5278/IJSEPM.2017.12.2>.
- [5] Lund H, Østergaard PA, Connolly D, Ridjan I, Mathiesen BV, Hvelplund F et al. Energy Storage and Smart Energy Systems. International Journal of Sustainable Energy Planning and Management 2016(11):3–14. <https://doi.org/10.5278/IJSEPM.2016.11.2>.
- [6] Askeland K, Johnsen Rygg B, Sperling K. The role of 4th generation district heating (4GDH) in a highly electrified hydropower dominated energy system. International Journal of Sustainable Energy Planning and Management 2020(27):17–34. <https://doi.org/10.5278/IJSEPM.3683>.
- [7] Tveten ÅG, Bolkesjø TF, Ilieva I. Increased demand-side flexibility: market effects and impacts on variable renewable energy integration. International Journal of Sustainable Energy Planning and Management 2016(11):33–50. <https://doi.org/10.5278/IJSEPM.2016.11.4>.
- [8] Roberto R, Iulio R de, Di Somma M, Graditi G, Guidi G, Noussan M. A multi-objective optimization analysis to assess the potential economic and environmental benefits of distributed storage in district heating networks: a case study. International Journal of Sustainable Energy Planning and Management 2019(20):5–20. <https://doi.org/10.5278/IJSEPM.2019.20.2>.

- [9] Prina MG, Cozzini M, Garegnani G, Moser D, Filippi Oberegger U, Vaccaro R et al. Smart energy systems applied at urban level: the case of the municipality of Bressanone-Brixen. International Journal of Sustainable Energy Planning and Management 2016(10):33–52. <https://doi.org/10.5278/IJSEPM.2016.10.4>.
- [10] Knies J. A spatial approach for future-oriented heat planning in urban areas. International Journal of Sustainable Energy Planning and Management 2018(16):3–30. <https://doi.org/10.5278/IJSEPM.2018.16.2>.
- [11] Heinisch V, Göransson L, Odenberger M, Johansson F. A city optimisation model for investigating energy system flexibility. International Journal of Sustainable Energy Planning and Management 2019(24):57–66. <https://doi.org/10.5278/IJSEPM.3328>.
- [12] Ommen T, Markussen WB, Elmegård B. Heat pumps in combined heat and power systems. Energy 2014(76):989–1000. <https://doi.org/10.1016/j.energy.2014.09.016>.
- [13] Levihn F. CHP and heat pumps to balance renewable power production: Lessons from the district heating network in Stockholm. Energy 2017(137):670–8. <https://doi.org/10.1016/j.energy.2017.01.118>.
- [14] Blarke M, Lund H. Large-scale heat pumps in sustainable energy systems: System and project perspectives. Therm sci 2007;11(3):143–52. <https://doi.org/10.2298/TSCI0703143B>.
- [15] EMD International A/S. energyPRO. [October 27, 2020]; Available from: <https://www.emd.dk/de/energypro/>.
- [16] Sneum DM, Sandberg E. Economic incentives for flexible district heating in the Nordic countries. International Journal of Sustainable Energy Planning and Management 2018(16):27–44. <https://doi.org/10.5278/IJSEPM.2018.16.3>.
- [17] Østergaard PA, Andersen AN. Variable taxes promoting district heating heat pump flexibility. Energy 2021(221):119839. <https://doi.org/10.1016/j.energy.2021.119839>.
- [18] Rämä M, Wahlroos M. Introduction of new decentralised renewable heat supply in an existing district heating system. Energy 2018(154):68–79. <https://doi.org/10.1016/j.energy.2018.03.105>.
- [19] Kontu K, Rinne S, Junnila S. Introducing modern heat pumps to existing district heating systems – Global lessons from viable decarbonizing of district heating in Finland. Energy 2019(166):862–70. <https://doi.org/10.1016/j.energy.2018.10.077>.
- [20] Bach B, Werling J, Ommen T, Münster M, Morales JM, Elmegård B. Integration of large-scale heat pumps in the district heating systems of Greater Copenhagen. Energy 2016(107):321–34. <https://doi.org/10.1016/j.energy.2016.04.029>.
- [21] Pieper H, Mašatin V, Volkova A, Ommen T, Elmegård B, Brix Markussen W. Modelling framework for integration of large-scale heat pumps in district heating using low-temperature heat sources. International Journal of Sustainable Energy Planning and Management 2019(20):67–86. <https://doi.org/10.5278/IJSEPM.2019.20.6>.
- [22] Popovski E, Aydemir A, Fleiter T, Bellstädt D, Büchele R, Steinbach J. The role and costs of large-scale heat pumps in decarbonising existing district heating networks – A case study for the city of Herten in Germany. Energy 2019(180):918–33. <https://doi.org/10.1016/j.energy.2019.05.122>.
- [23] Jesper M, Schlosser F, Pag F, Walmsley TG, Schmitt B, Vajen K. Large-scale heat pumps: Uptake and performance modelling of market-available devices. Renewable and Sustainable Energy Reviews 2021(137):110646. <https://doi.org/10.1016/j.rser.2020.110646>.
- [24] Bundesamt für Wirtschaft und Ausfuhrkontrolle. Bundesförderung für effiziente Wärmenetze (Wärmenetzsysteme 4.0). [October 20, 2020]; Available from: https://www.bafa.de/DE/Energie/Energieeffizienz/Waermenetze/waermenetze_node.html.
- [25] Pohlmann Paperback of Refrigeration Technology: Basics, applications, working tables and regulations. 22nd ed. Berlin: VDE VERLAG; 2018 (in German).
- [26] Arpagaus C. High-temperature heat pumps: Market overview, state of the art and application potentials. Berlin, Offenbach: VDE Verlag GmbH; 2019 (in German).
- [27] Schlosser F, Jesper M, Vogelsang J, Walmsley TG, Arpagaus C, Hesselbach J. Large-scale heat pumps: Applications, performance, economic feasibility and industrial integration. Renewable and Sustainable Energy Reviews 2020(133):110219. <https://doi.org/10.1016/j.rser.2020.110219>.
- [28] Østergaard PA, Andersen AN. Booster heat pumps and central heat pumps in district heating. Applied Energy 2016(184):1374–88. <https://doi.org/10.1016/j.apenergy.2016.02.144>.
- [29] Meteotest AG. Meteonorm. [October 29, 2020]; Available from: <https://meteonorm.com/>.
- [30] Hellwig M. Development and application of parameterised standard load profiles [PhD Thesis]. München: TU München; 2003 (in German).
- [31] Hinterstocker M, Eberl B, Roon Sv. Further development of the standard load profile method gas. München: Forschungsgesellschaft für Energiewirtschaft mbH (FfE); 2015 (in German); Available from: https://www.bdew.de/media/documents/201507_Weiterentwicklung-SLP-Gas.pdf. [November 14, 2020].
- [32] Oeko-Institut. EEG-Calculator.: Calculation and scenario model to determine the EEG levy (V 4.1.1). [November 03, 2020]; Available from: <https://www.agora-energiewende.de/veroeffentlichungen/eeg-rechner-fuer-excel/>.
- [33] Baez MJ, Larriba Martinez T. Technical Report on the Elaboration of a Cost Estimation Methodology: Work Package

- 3 - Estimating RHC energy costs. Madrid, Spain: Creara; 2015; Available from: <https://www.front-rhc.eu/library/>. [May 12, 2021].
- [34] Große R, Binder C, Wöll S, Geyer R, Robbi S. Study on long term projections of large-scale heating and cooling in the EU. Luxembourg: European Union; 2017. <https://doi.org/10.2760/24422>.
- [35] Danish Energy Agency and Energinet. Technology Data (Update April 2020): Generation of Electricity and District heating. Copenhagen; 2016; Available from: [https://ens.dk/files/Statistik/technology_data_catalogue_for_el_and_dh_-0009.pdf](https://ens.dk/sites/ens.dk/files/Statistik/technology_data_catalogue_for_el_and_dh_-0009.pdf). [March 17, 2021].
- [36] Meesenburg W, Markussen WB, Ommen T, Elmegaard B. Optimizing control of two-stage ammonia heat pump for fast regulation of power uptake. *Applied Energy* 2020(271):115126. <https://doi.org/10.1016/j.apenergy.2020.115126>.
- [37] Meesenburg W. Heat pumps supplying district heating and ancillary services for the power system [PhD Thesis]. Kongens Lyngby: Technical university of Denmark. DCAMM Special Report; 2020.
- [38] Ommen T, Jensen JK, Meesenburg W, Jørgensen PH, Pieper H, Markussen WB et al. Generalized COP estimation of heat pump processes for operation off the design point of equipment. Proceedings of the 25th IIR International Congress of Refrigeration 2019(648). <https://doi.org/10.18462/iir.icr.2019.0648>.
- [39] Lund PD, Lindgren J, Mikkola J, Salpakari J. Review of energy system flexibility measures to enable high levels of variable renewable electricity. *Renewable and Sustainable Energy Reviews* 2015(45):785–807. <https://doi.org/10.1016/j.rser.2015.01.057>.
- [40] Kirkerud JG, Trømborg E, Bolkesjø TF. Impacts of electricity grid tariffs on flexible use of electricity to heat generation. *Energy* 2016(115):1679–87. <https://doi.org/10.1016/j.energy.2016.06.147>.
- [41] Trømborg E, Havskjold M, Bolkesjø TF, Kirkerud JG, Tveten ÅG. Flexible use of electricity in heat-only district heating plants. *International Journal of Sustainable Energy Planning and Management* 2017(12):29–46. <https://doi.org/10.5278/IJSEPM.2017.12.4>.
- [42] Østergaard PA, Johannsen RM, Lund H, Mathiesen BV. Developments in 4th generation district heating and smart energy systems. *International Journal of Sustainable Energy Planning and Management* 2021;x. <https://doi.org/10.5278/ijsepm.6432>.

